University of Stuttgart
Germany

EPR Imaging Concept Based on a VCO Array Architecture

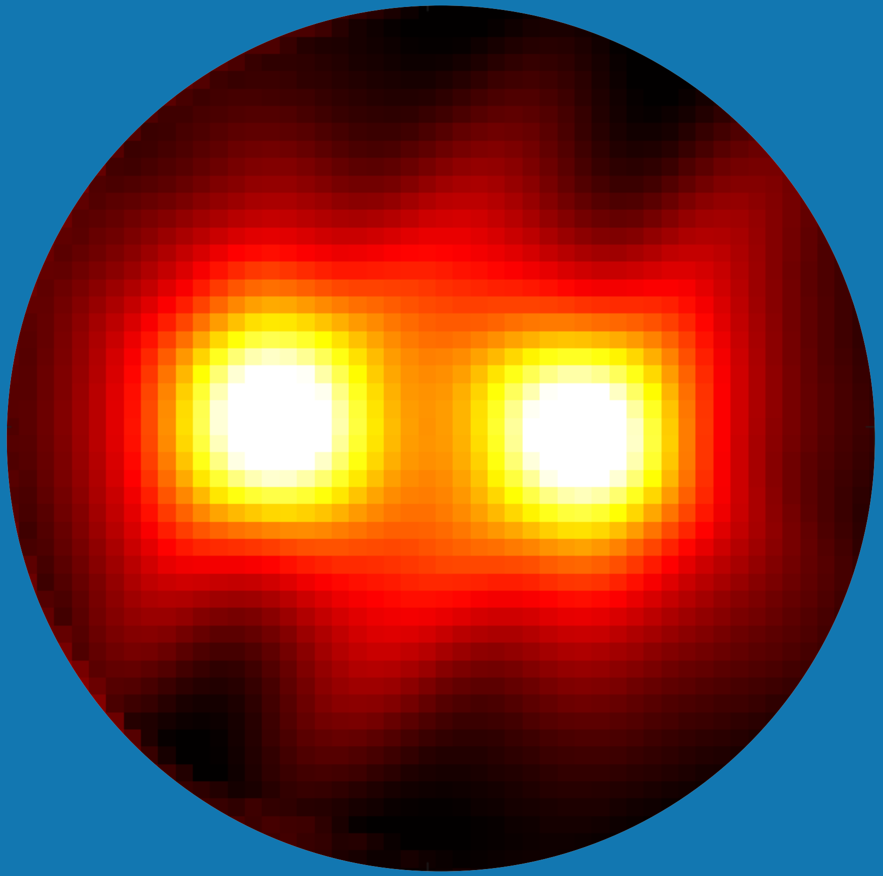

Weiyi Zhang

Master’s Thesis – Final Presentation

Supervisor: M. Sc. Zhibin Zhao

02/09/2026

Outline

- Motivation
- Experimental setup
  - VCO-based EPR probehead
  - Gradient coils and current driver
- Spatial - spatial imaging
- Spectral - spatial imaging
- Summary and outlook

MOTIVATION

Motivation

- Why extending our NMR probe toward VCO-based EPR imaging?
  - Complementary insights to NMR, sensitive to functional and microenvironment-related properties.
  - No previous demonstration of VCO-based EPR imaging

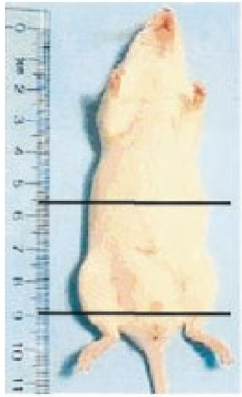

photograph of the mouse

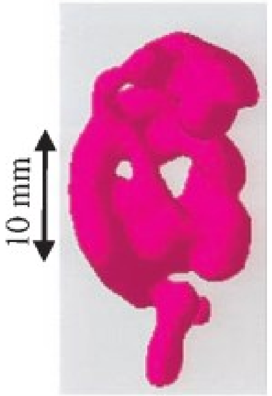

Spatial-spatial image

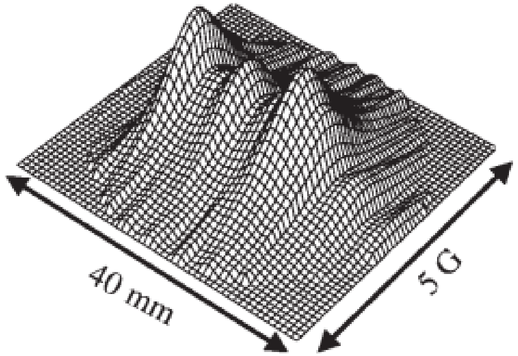

spectral-spatial image

(Source: He et al., *Proc. Natl. Acad. Sci. USA*, 1999)

- Why does our probe design have potential for imaging?
  - Planar coil with 13 mm in diameter, offering a sufficient field-of-view for imaging
  - The ultra-low operating field allows deeper penetration into living tissue

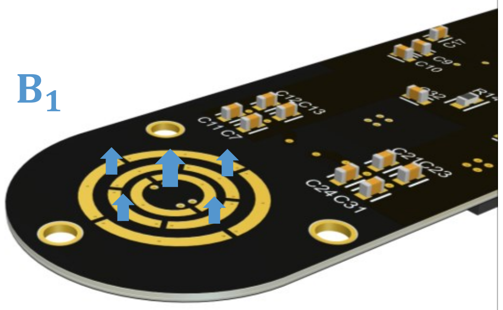

Motivation

- Functional information in EPR is encoded in spectral properties, such as linewidth

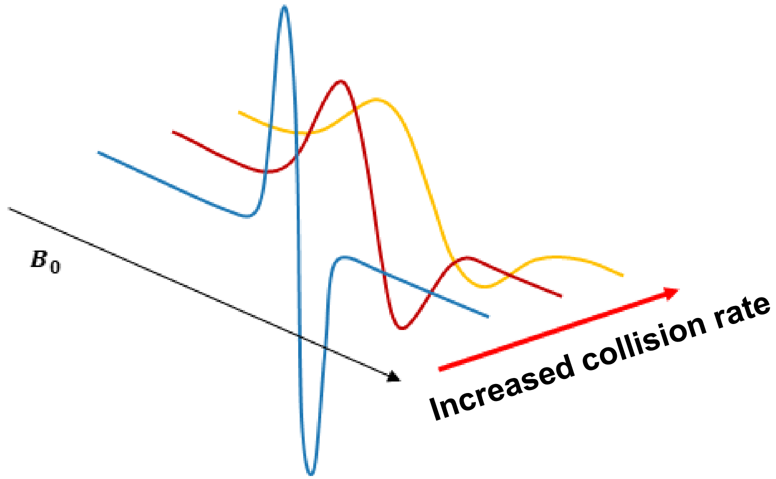

- Previously measured oxygen dependence of linewidth (Sample: LiNc-BuO)

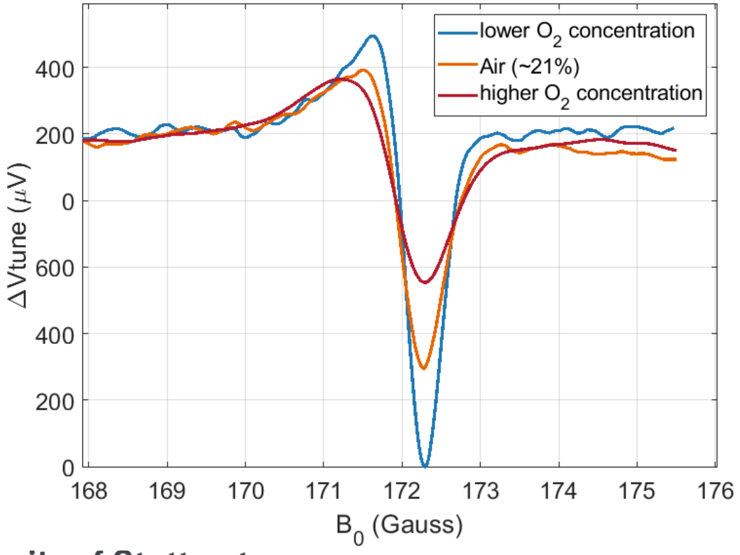

	Lower O2	Air (~21%)	Higher O2
Linewidth	664 ±19.4 mG	774 ±14.5 mG	1080 ± 22.5 mG
Amplitude	613.2 μV	447.9 μV	212.4 μV

Linewidth broadens with increasing pO_2

EXPERIMENTAL SETUP

Experimental setup

- VCO-based CW-EPR setup

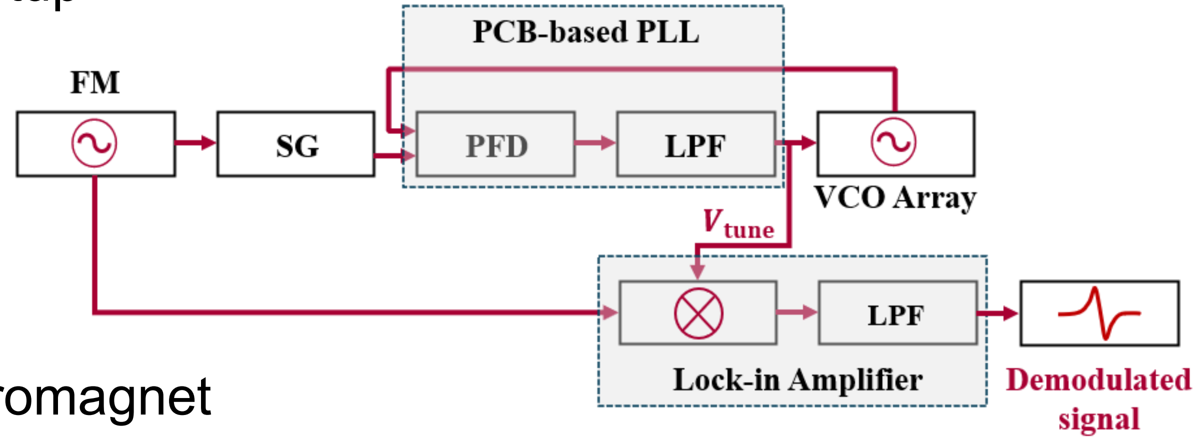

- System setup with electromagnet

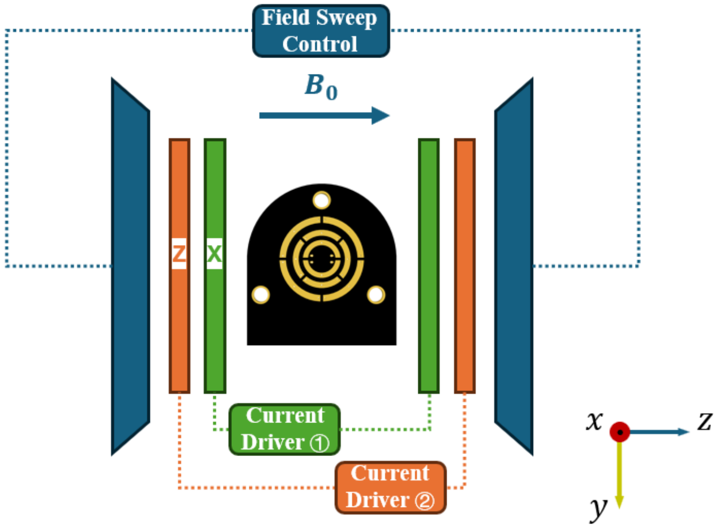

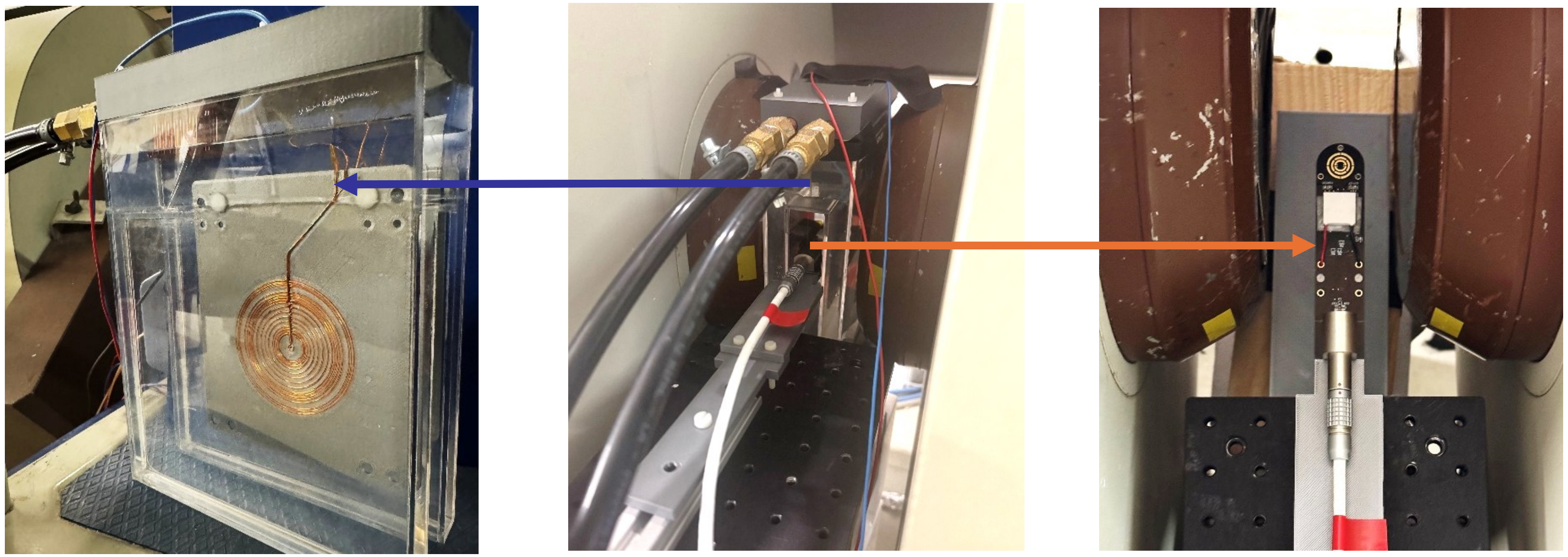

VCO-BASED EPR PROBE HEAD

VCO-based EPR probe head

- Probe head architecture: chip-integrated VCO array, planar segmented coil and PCB-based PLL

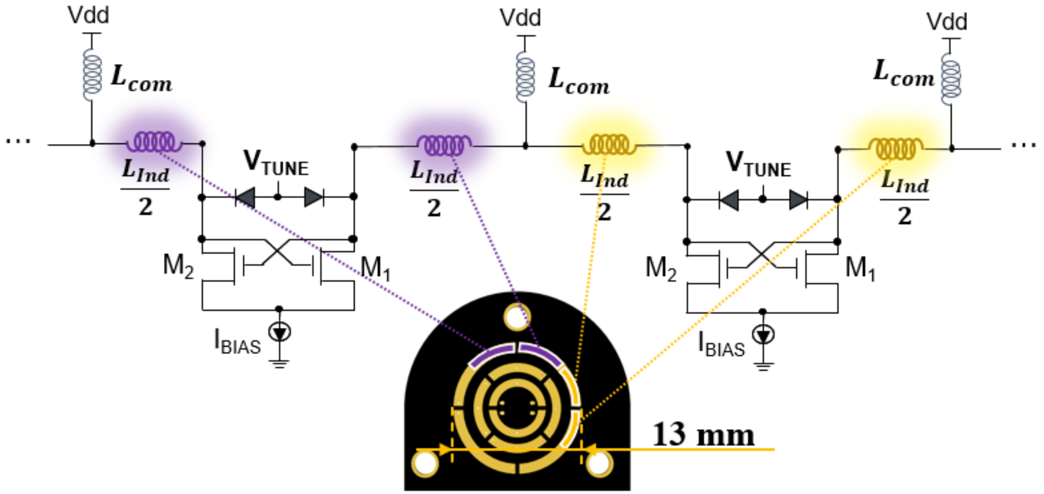

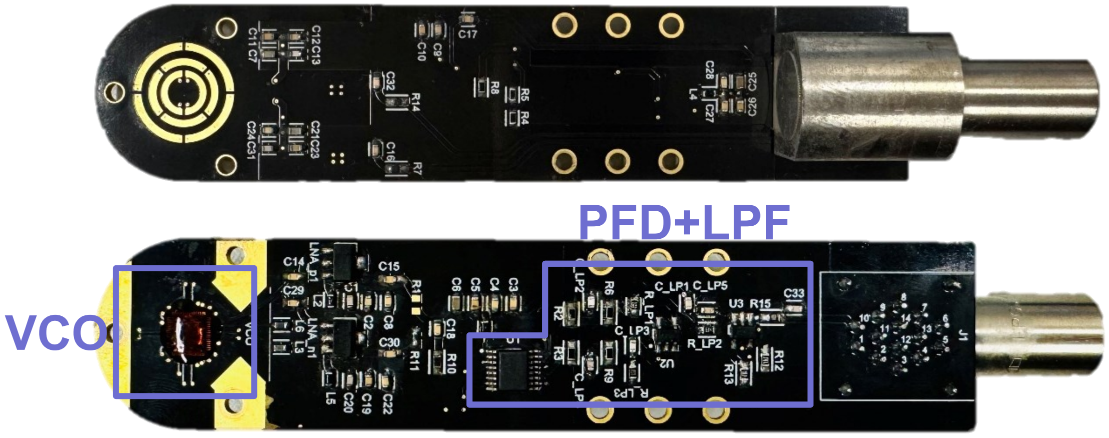

- Phase noise: -101 dBc/Hz @100kHz
- PLL closed-loop Bandwidth: 3.2 MHz (-3 dB Gain)
- VCO gain: 3.7 V/MHz
- Lock range: 473.5 MHz – 481.5 MHz
- Selected working frequency: 478.6 MHz (~171Gauss)

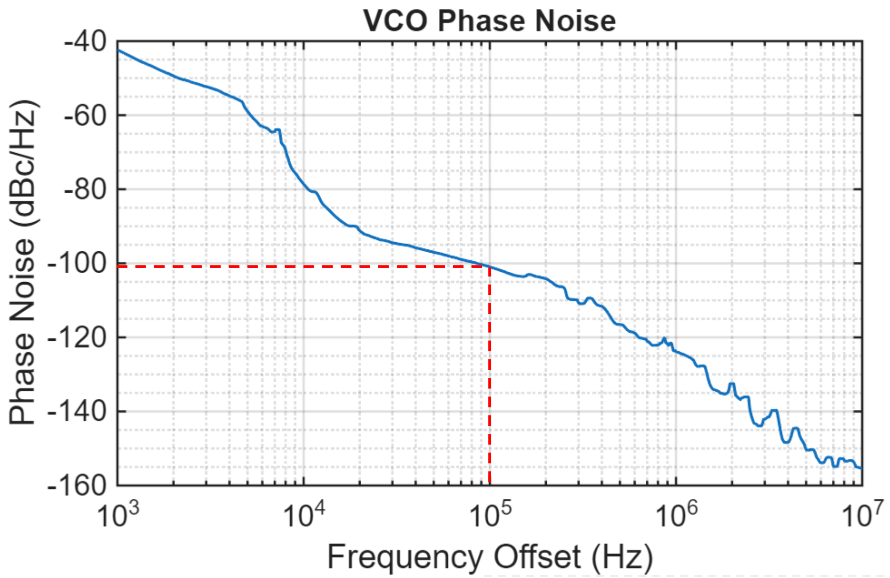

GRADIENT COILS AND CURRENT DRIVER

Gradient coils

- Bi-planar gradient coils: Y- and Z-directions
- Coil separation (gap): $40\ \mathrm{mm}$
- Coil diameter: $60\ \mathrm{mm}$
- Region of interest (ROI): $x = \pm 2.5\ \mathrm{mm}, y = \pm 5.0\ \mathrm{mm}, z = \pm 5.0\ \mathrm{mm}$
- Design evolution:
  - 2-layer PCB (single pair) → 4-layer PCB (double pairs) → handmade with copper-wire (double pairs)

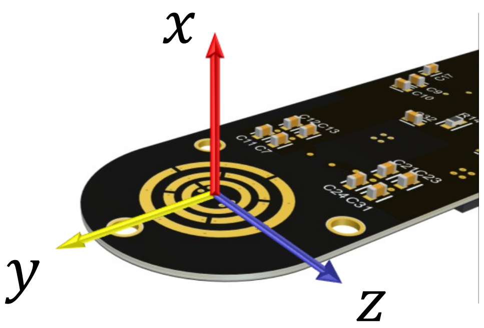

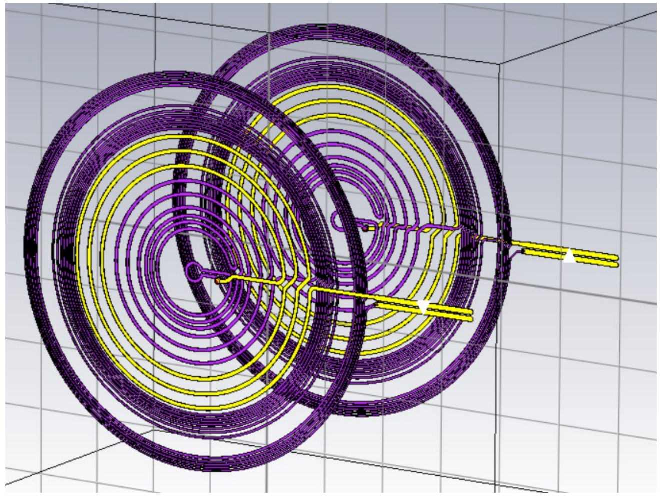

Z-Gradient

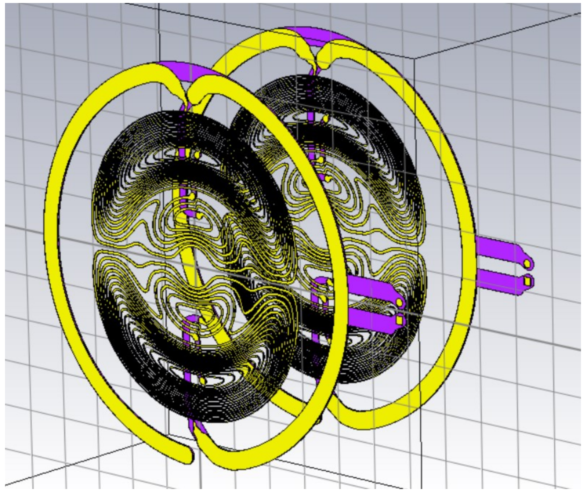

Y-Gradient

Gradient coils

- Y-Gradient coil ver.1
  - **PCB** fabrication (2 oz copper), **single side**
    - Gradient sensitivity: $10.0\ \mu T/mm/A$
    - RMS nonlinearity (ROI) : $0.65\ \%$
    - Resistance: 5.8 Ω per coil, 11.6 Ω total

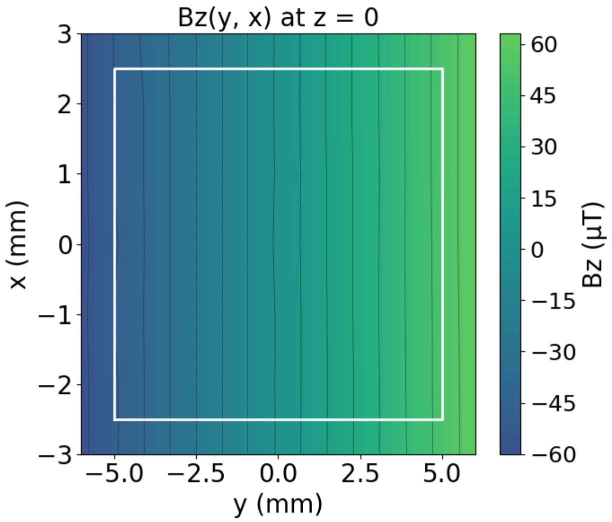

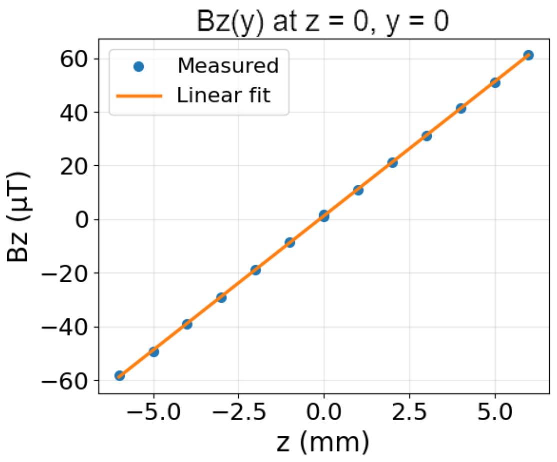

- Y-Gradient coil ver.2
  - **PCB** fabrication (2 oz copper), **double sides**
    - Gradient sensitivity : $18.9\ \mu T/mm/A$
    - RMS nonlinearity (ROI) : $0.59\ \%$
    - Resistance: 5.7 Ω per coil, 22.8 Ω total

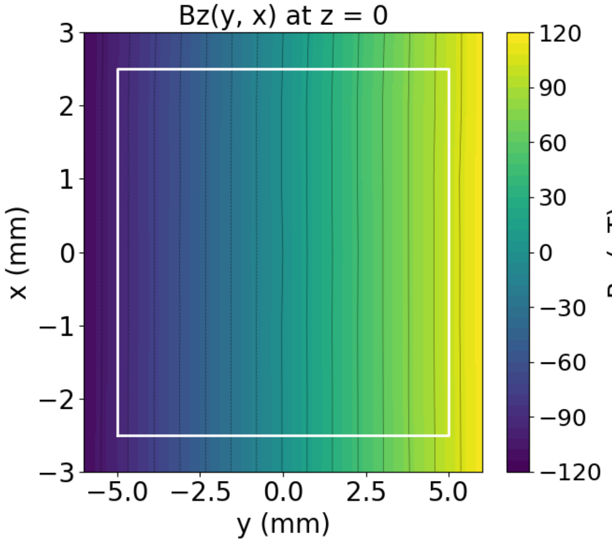

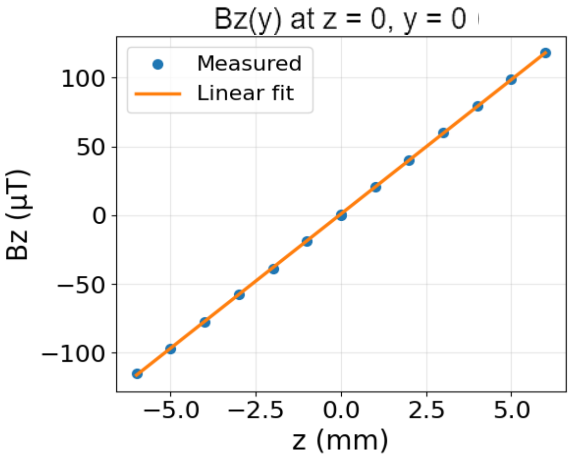

Gradient coils

- Y-Gradient coil ver.3
  - **0.3 mm copper wire, double sides**
    - Gradient sensitivity: $21.8\ \mu T/mm/A$
    - RMS nonlinearity (ROI) : $0.74\ \%$
    - Resistance: 1.2 Ω per coil, 4.8 Ω total

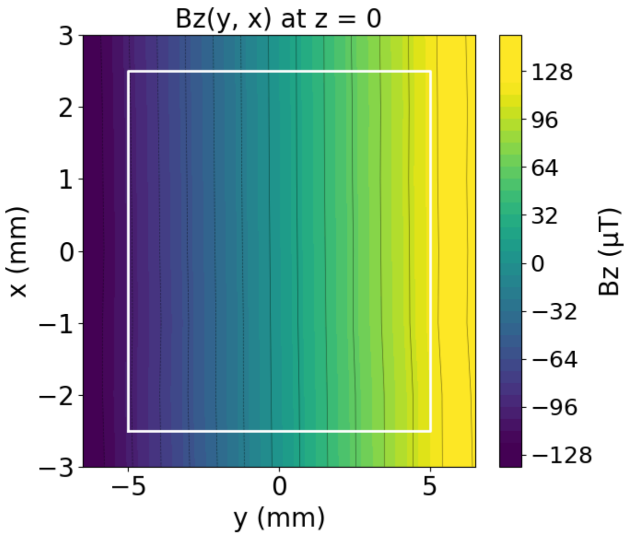

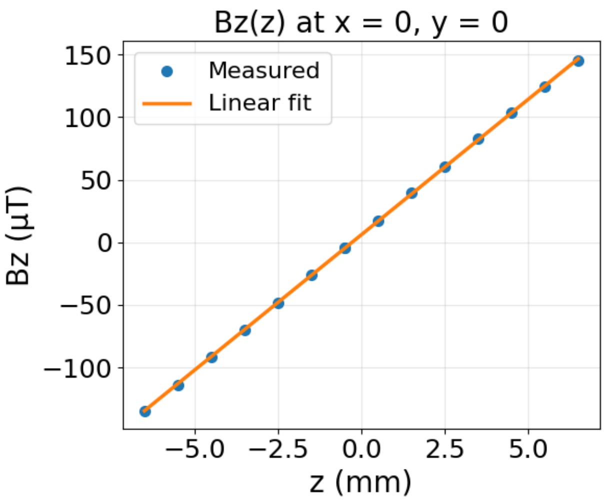

- Summary for Y-Gradient coil versions

	Gradient sensitivity	RMS nonlinearity	Resistance
2-layer PCB (single pair)	$10.0\ \mu T/mm/A$	$0.65\ \%$	11.6 ohm
4-layer PCB (double pairs)	$18.9\ \mu T/mm/A$	$0.59\ \%$	22.8 ohm
copper-wire coils (double pairs)	$21.8\ \mu T/mm/A$	$0.74\ \%$	4.8 ohm

Gradient coils

- Z-Gradient coils
  - 0.6 mm copper wire, double sides
  - Gradient sensitivity: $14\ \mu T/mm/A$ (Gap $40\ mm$), $13.1\ \mu T/mm/A$ (Gap $48\ mm$)
  - RMS nonlinearity (ROI) : $0.81\ \%$
  - Resistance: 0.2 Ω per coil, 0.8 Ω total

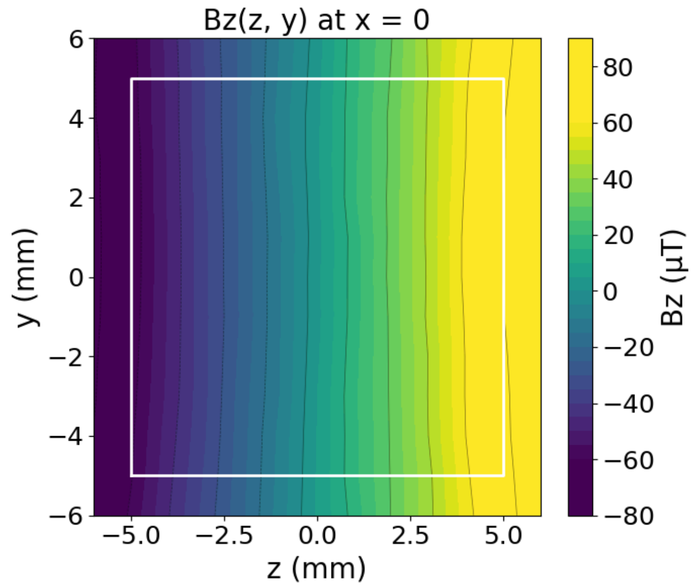

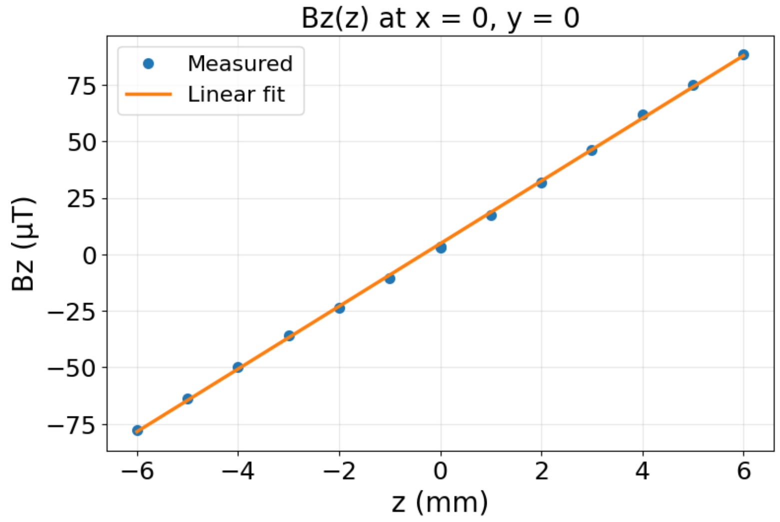

Current driver

- Current Driver: Push-pull (OPA549S)
- Large coil separation → high current required for sufficient gradient strength
- Output current limit: $8\ \mathrm{A}$ Continuous, $10\ \mathrm{A}$ Peak
- CW-EPR operation → DC current output required

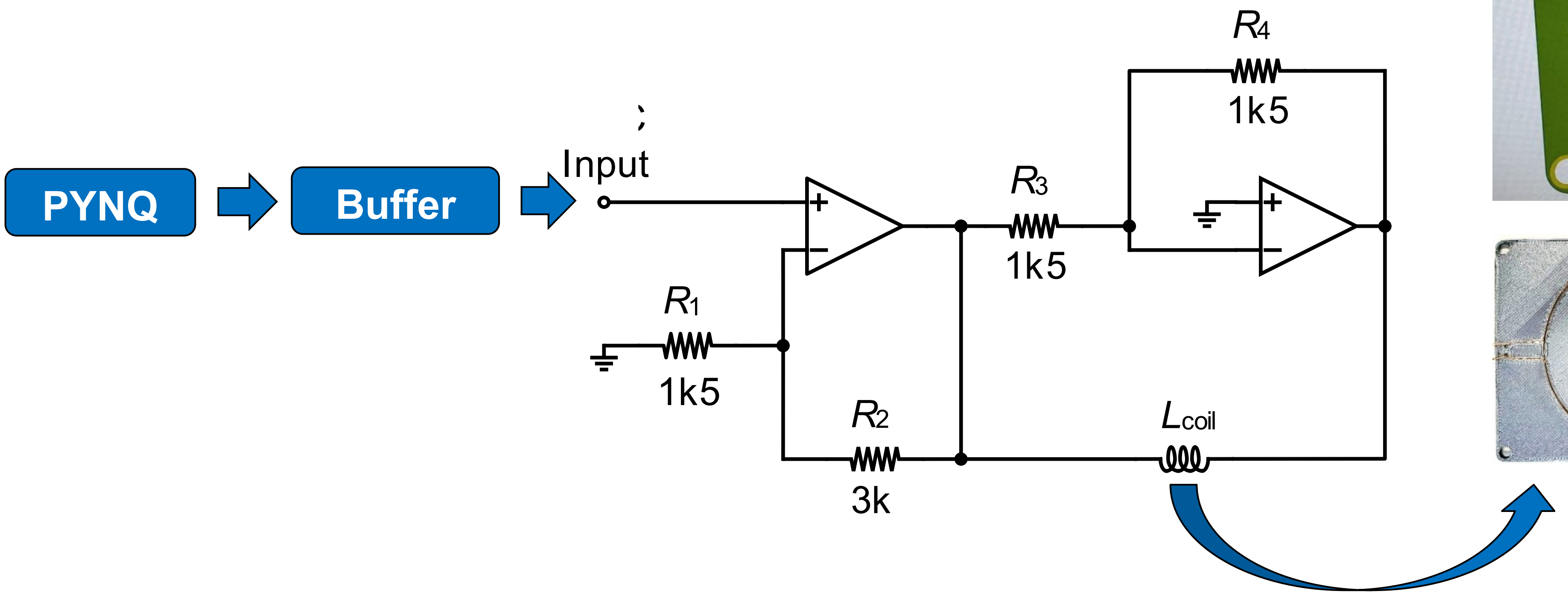

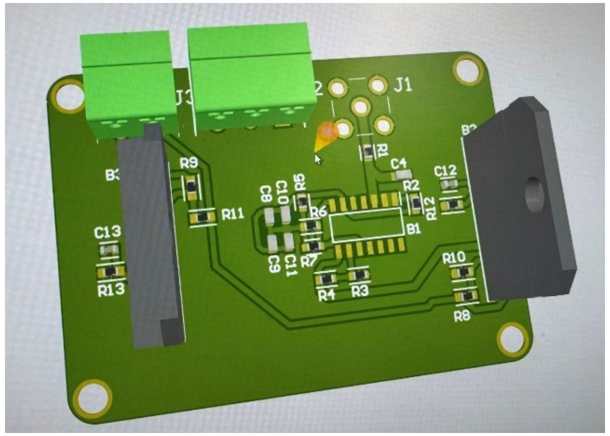

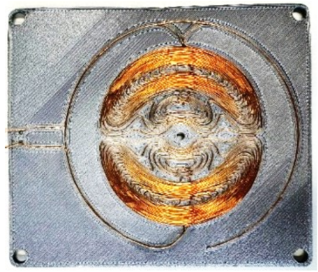

SPATIAL-SPATIAL IMAGING

Spatial-spatial principle

- 2D Spatial–Spatial CW-EPRI: Radon Transform and Reconstruction
  - Forward model (with gradient Y and Z):

$$\boxed{P(s,\theta_i)} = \iint \boxed{f(y,z)}\, \boxed{\delta(s - y\sin\theta_i - z\cos\theta_i)}\, dydz$$

We measured

We want

$\delta(\cdot)$ mathematically encodes the physical resonance condition

- Projection coordinate s
  - Each measured CW-EPR signal corresponds to a projection along the coordinate s
  - Lines of integration: $s = y\sin\theta_i + z\cos\theta_i$
  - The projection angle θ_i is defined by the gradient direction
  - Sampled uniformly in $\theta_i \in [0,\pi)$

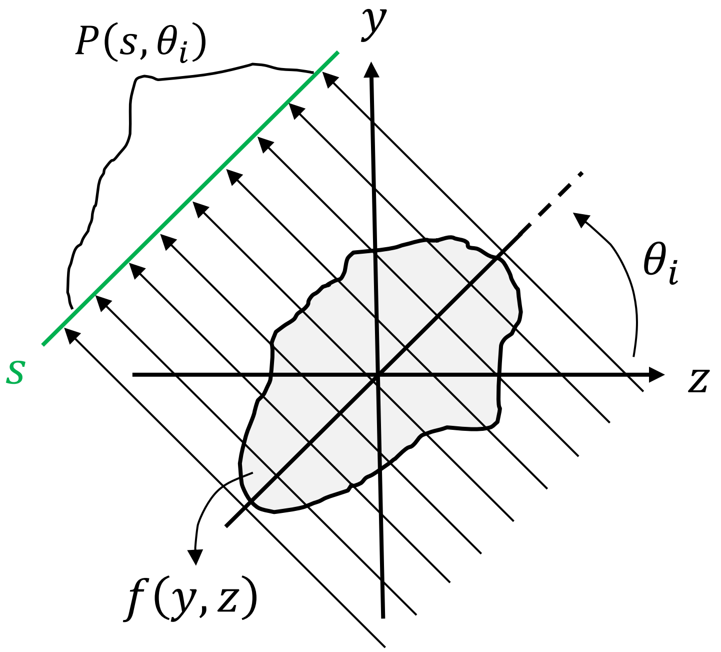

Spatial-spatial principle

- 2D Spatial–Spatial CW-EPRI: Radon Transform and Reconstruction
  - Forward model (with gradient Y and Z):

$$\boxed{P(s,\theta_i)} = \iint \boxed{f(y,z)}\,\boxed{\delta(s - y\sin\theta_i - z\cos\theta_i)}\,dydz$$

We measured

We want

$\delta(\cdot)$ mathematically encodes the physical resonance condition

- Resonance condition in CW-EPR: Position-dependent resonance field
  - $B_{res}(\boldsymbol{r}) = B_0 + \Delta B(\boldsymbol{r}) = B_0 + G_y y + G_z z$

- Changing the gradient field strength → projections at different angles

$$\begin{cases} G_y(\theta_i) = G_0 \sin\theta_i \\ G_z(\theta_i) = G_0 \cos\theta_i \end{cases} \Rightarrow \Delta B(\boldsymbol{r}) = G_0(\mathrm{y}\sin\theta_i + z\cos\theta_i) = G_0 s$$

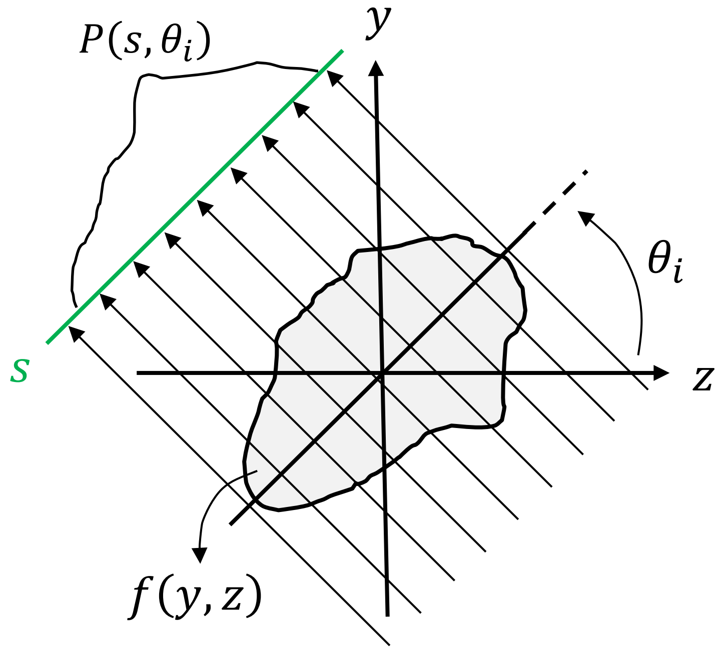

Spatial-spatial principle

- First measurement for spatial-spatial (sample: DPPH)
  - Gradient Y sensitivity $\mathrm{S_y}$: $18.9\ \mu\mathrm{T/mm/A}$
  - Gradient Z sensitivity $\mathrm{S_z}$: $13.1\ \mu\mathrm{T/mm/A}$
  - Projections number: $N = 16$
  - $I_{\mathrm{y\_max}} = 2.0\ \mathrm{A}$

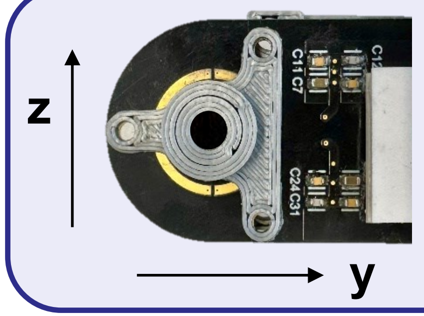

- single cylinder
- diameter of 4 mm

$$\begin{cases} G_y(\theta_i) = G_0 \sin\theta_i \\ G_z(\theta_i) = G_0 \cos\theta_i \end{cases} \Rightarrow \begin{cases} G_y(\theta_i) = \mathrm{S_y} I_y(\theta_i) \\ G_z(\theta_i) = \mathrm{S_z} I_z(\theta_i) \end{cases}$$

$$\boxed{|G_0| = \sqrt{(G_y)^2 + (G_z)^2} = \mathrm{const} = 37.8\ \mathrm{uT/mm}}$$

N	θ_i (deg)	$G_y(\theta_i)$ (μT/mm)	$G_z(\theta_i)$ (μT/mm)
1	5.625	3.78	37.7
2	16.875	11.0	36.2
3	28.125	17.8	33.4
…	…	…	…
14	151.875	17.8	−33.4
15	163.125	11.0	−36.2
16	174.375	3.78	−37.7

Phase correction

- Phase correction before reconstruction

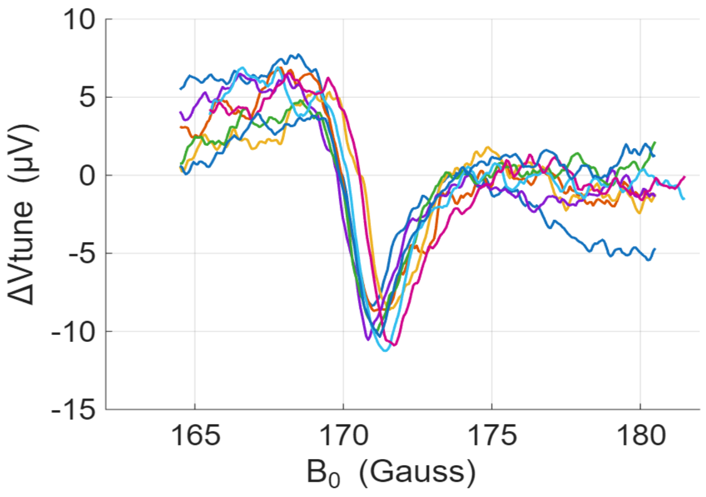

  – mixture of absorption and dispersion
  – Pure absorption is the most robust and commonly used input for CW-EPRI reconstruction.

– $S(B) = aA'(B) + bD'(B) + c_0 + c_1 B$

- $A'(B)$: first derivative of absorption lineshape
- $D'(B)$: first derivative of dispersion lineshape
- a, b: mixing coefficients (effective phase-dependent)
- $c_0 + c_1 B$: baseline offset and linear drift

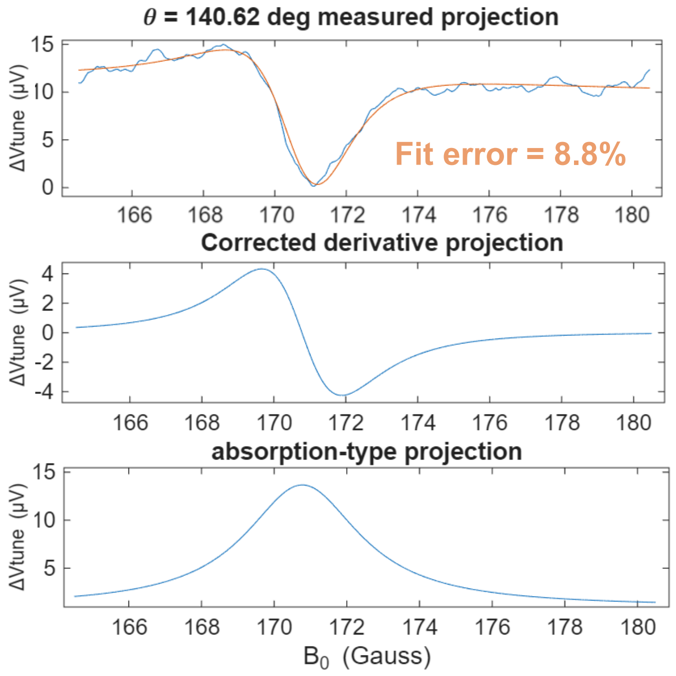

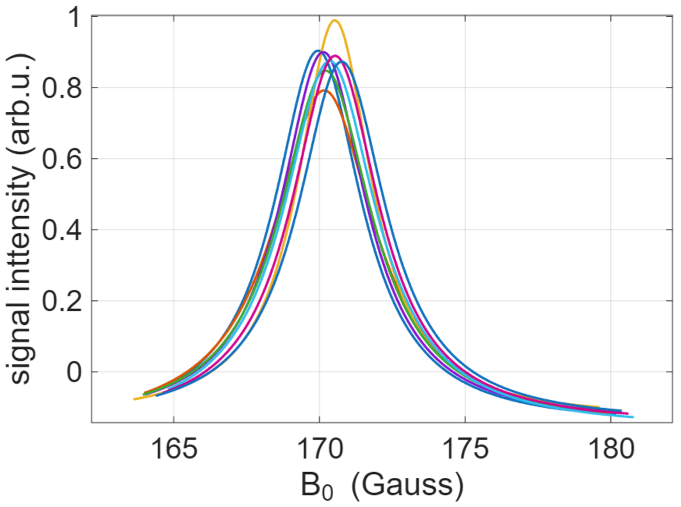

Spatial-spatial image results

- Image reconstruction: Deconvolution by Filtered Backprojection (FBP)

$$P(s,\theta_i) = \iint \boxed{f(y,z)}\, \delta(s - y\sin\theta_i - z\cos\theta_i)\, dydz \;\Longrightarrow\; \boxed{f(y,z)} = \frac{1}{N}\sum_{i=1}^{N} P^*(s = y\sin\theta_i + z\cos\theta_i, \theta_i)$$

  – P^*: filtered measured projections (Ram–Lak)

- Spatial-spatial image result

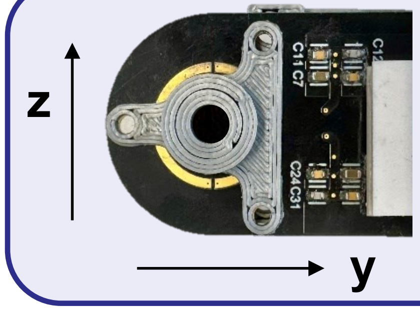

- single cylinder
- diameter 4 mm

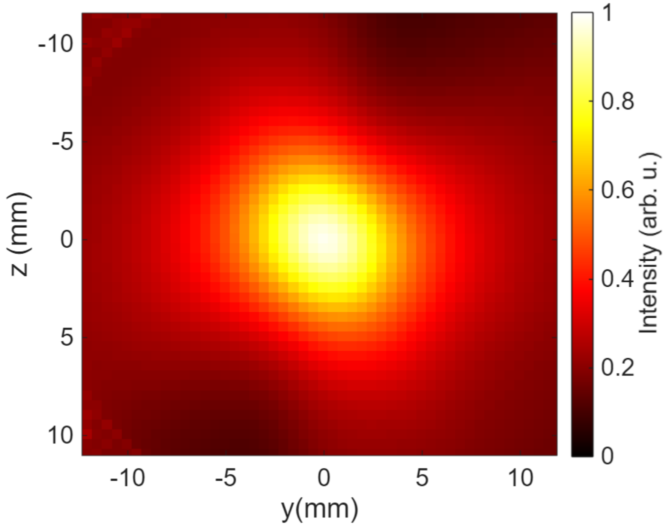

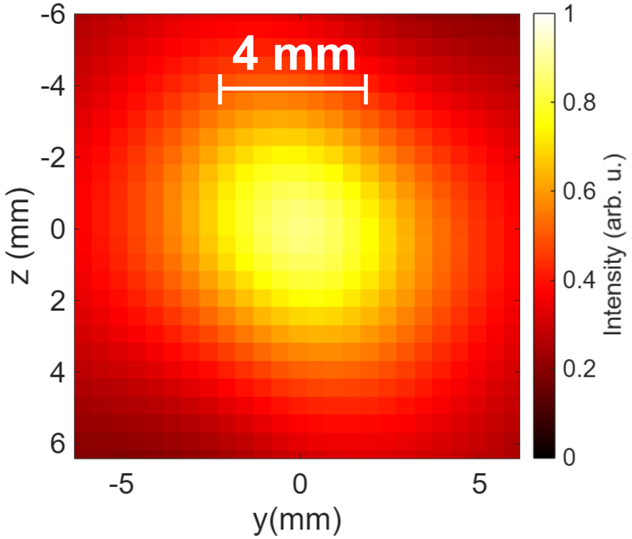

- Spatial Resolution: $\delta x \approx \frac{\Delta B_{pp}}{|G_0|}$

– S. S. Eaton and G. R. Eaton, Electron Spin Resonance 17, 109–129 (2000).
– Poole, C. P. – Electron Spin Resonance, 2nd ed.

Spatial-spatial image results

- Second measurement for spatial-spatial imaging

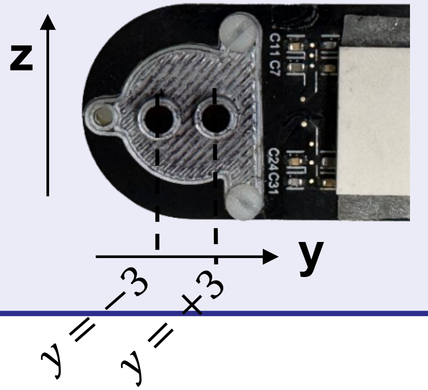

- Two cylinders, diameter of 3 mm
- Positioned symmetrically at y = ±3 mm

- Sample: DPPH
- Gradient Y: $21.8\ \mu\mathrm{T/mm/A}$
- Gradient Z: $13.1\ \mu\mathrm{T/mm/A}$
- $\mathrm{N} = 24$
- $I_{y\_\max} = 4.2\ \mathrm{A}$

$|G_0| = \mathrm{const} = 91.7\ \mathrm{uT/mm}$

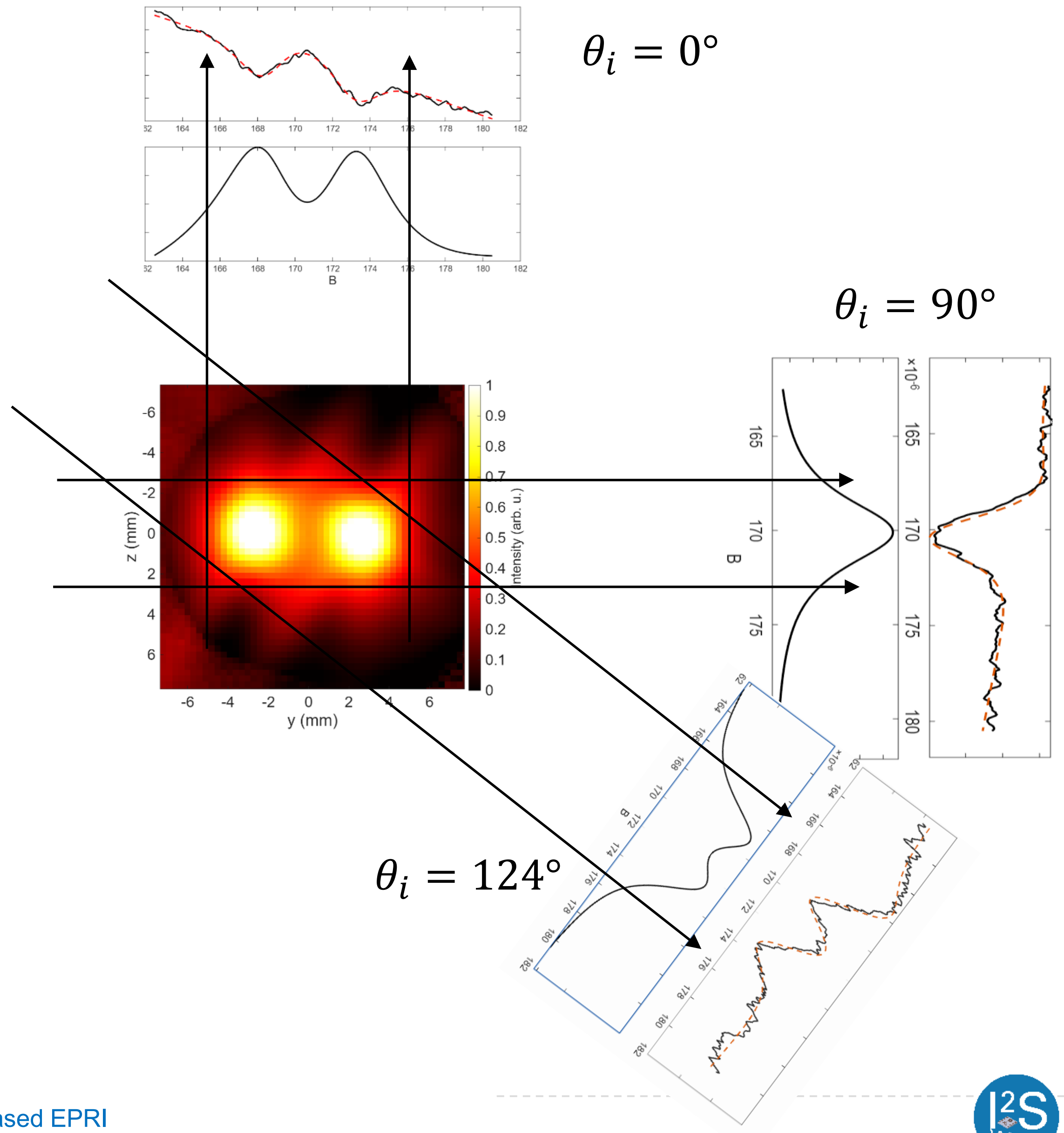

Spatial-spatial image results

- Second measurement for spatial-spatial imaging

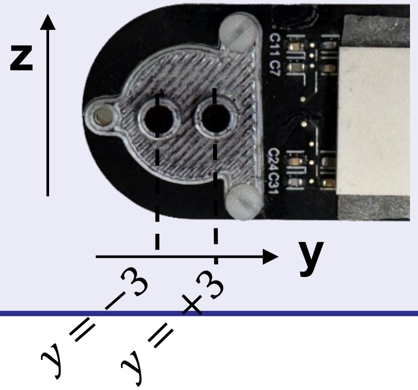

- Two cylinders, diameter of 3 mm
- Positioned symmetrically at y = ±3 mm

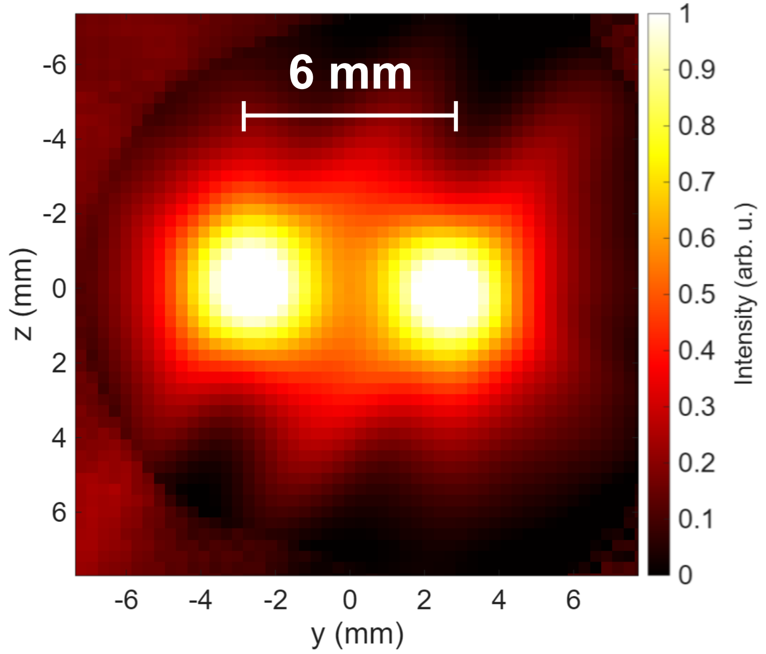

- Sample: DPPH
- Gradient Y: $21.8\ \mu T/mm/A$
- Gradient Z: $13.1\ \mu T/mm/A$
- $N = 24$
- $I_{y\_max} = 4.2\ A$

$$|G_0| = \mathrm{const} = 91.7\ \mathrm{uT/mm}$$

- Resolution: $\delta x \approx \frac{\Delta B_{pp}}{|G_0|} = \frac{194.1\mu T}{91.7\mu T/mm} \approx 2.1\ mm$

SPECTRAL-SPATIAL IMAGING

Spectral-spatial principle

- **2D Spectral–Spatial** imaging principle
  - Image function: $f(z,B)$ (with Z-gradient)
    - Spatial axis: z
    - Spectral axis: magnetic field B
  - Forward model (with Z-gradient)

Resonance condition: $B_0 = B + G_\alpha z$

$$\boxed{P(B_0)} = \iint \boxed{f(z,B)}\,\boxed{\delta(B_0 - B - G_\alpha z)}\, dB dz$$

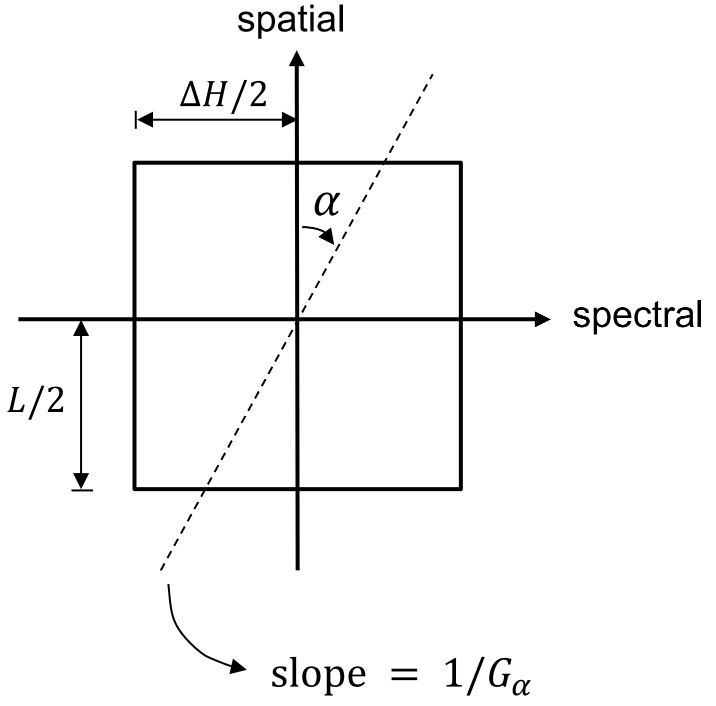

  - Spectral–spatial mixing angle α:

$$\tan\alpha = \frac{G_\alpha L}{\Delta H}$$

    - α depends on the applied gradient G_α, the spatial window (FOV) L, and the spectral window ΔH
    - $\alpha \in (-\pi/2, +\pi/2)$, non-uniform, more projections with large angels required

Spectral-spatial principle

- **2D Spectral–Spatial** imaging principle
  - Field sweep width:

$$\Delta B_{\text{sweep}} = \frac{\sqrt{2}\Delta H}{\cos \alpha}$$

    - Indicates the sweep range of B_0
    - Different sweep widths are required for different projections

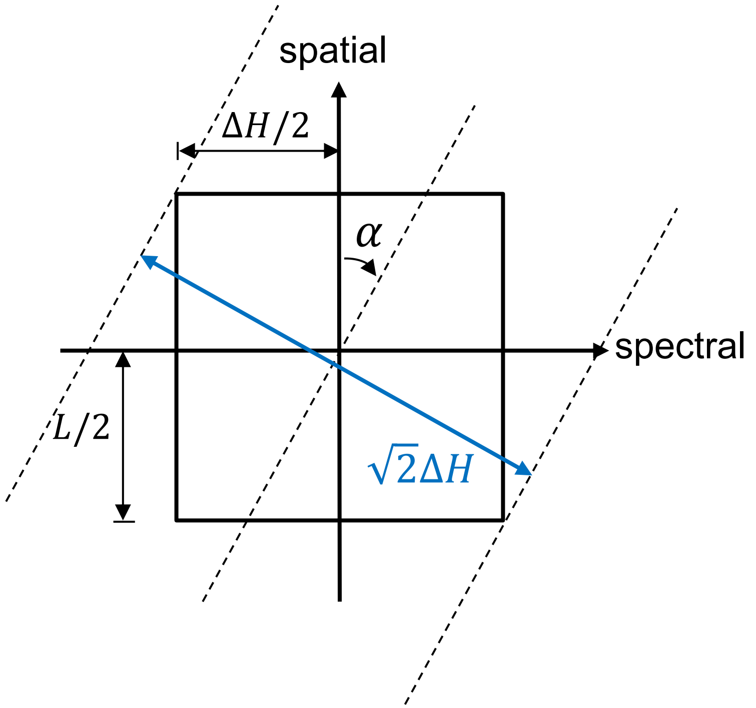

  - Image reconstruction
    - Reconstruction is performed using a iterative ART (Algebraic Reconstruction Technique)
    - ART is an iterative reconstruction method that updates the image by enforcing consistency with each measured projection.
    - **Robust to limited projections, non-uniform projection angels and higher experimental noise**

Spectral-spatial measurement results

- Spectral – spatial measurement (oxygen sensing sample: LiNc-BuO)
  - Spatial window (FOV): $\mathrm{L} = 12\ \mathrm{mm}$
  - Z-Gradient applied: $14\ \mu\mathrm{T/mm/A},\ \mathrm{I_{max}} = 5\ \mathrm{A}$
  - $|\mathrm{G_{max}}| = 70\ \mathrm{uT/mm}$
  - Maximum projection angel: $\alpha_{\max} = 70.3°$

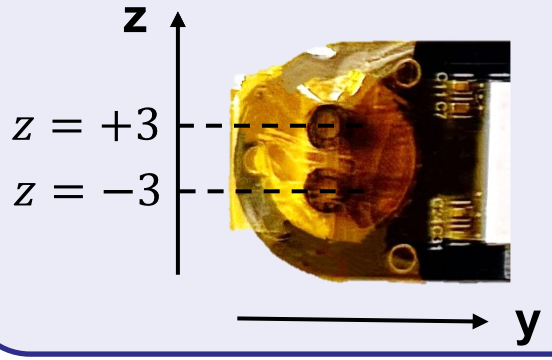

- Two cylinders, diameter d = 2.5 mm
- Positioned symmetrically at z ≈ ±3 mm

- Measured CW-EPR projections $(\mathrm{I} \geq 0)$

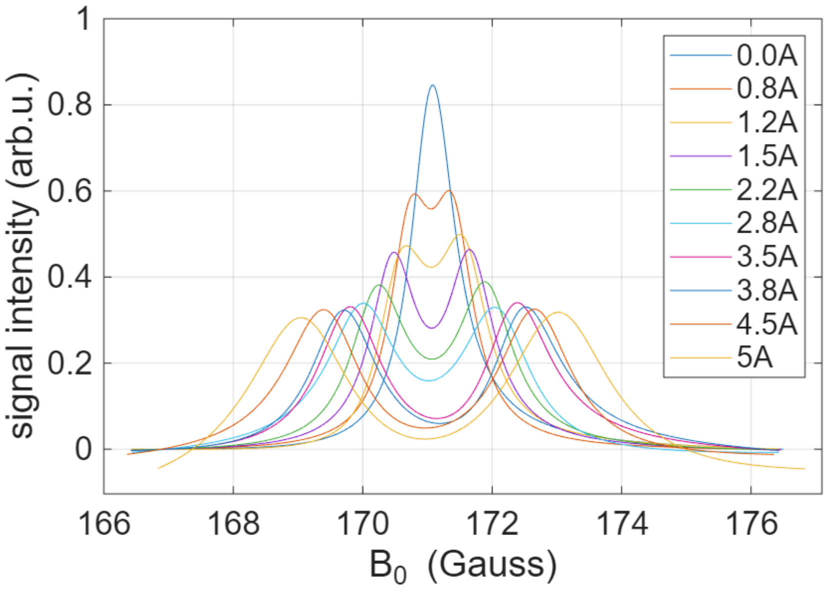

- Spectral–spatial sinogram

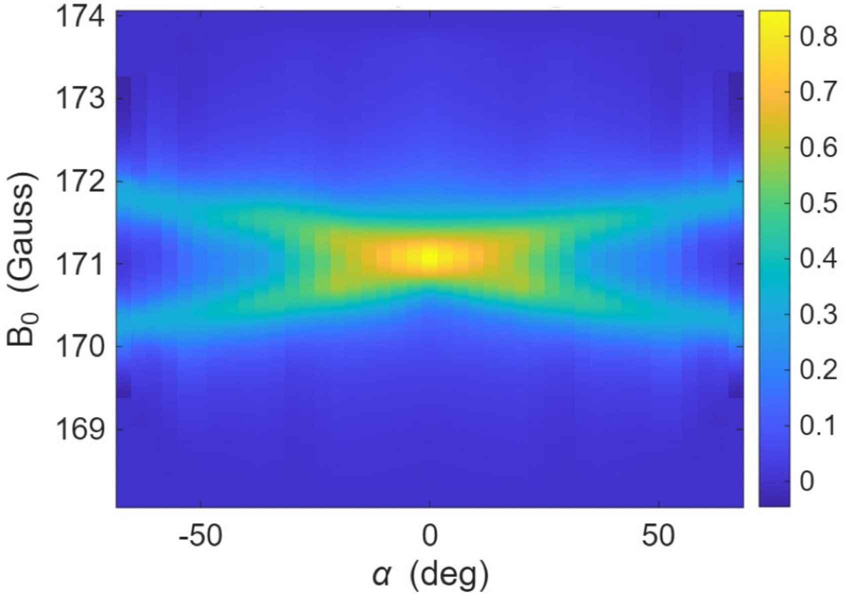

Spectral-spatial measurement results

- Spectral–spatial image reconstruction
  - reconstructed spectral–spatial distribution $f(z, B)$
  - $f(z, B)$ visualized in 3D

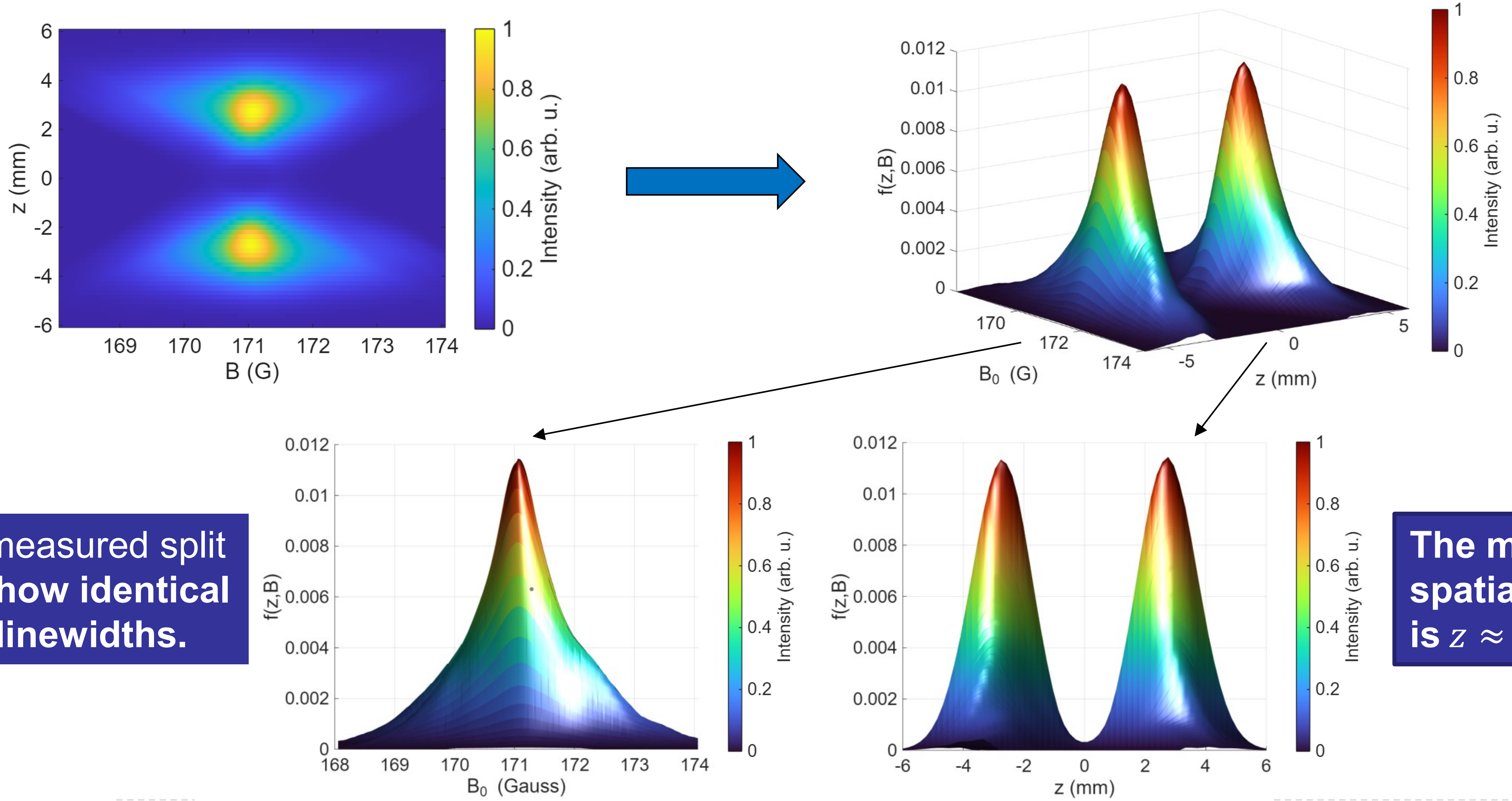

The two measured split spectra show identical spectral linewidths.

The measured spatial separation is $z \approx \pm 2.8\ mm$.

Spectral-spatial measurement results

- Local spectral linewidth extracted from reconstructed image

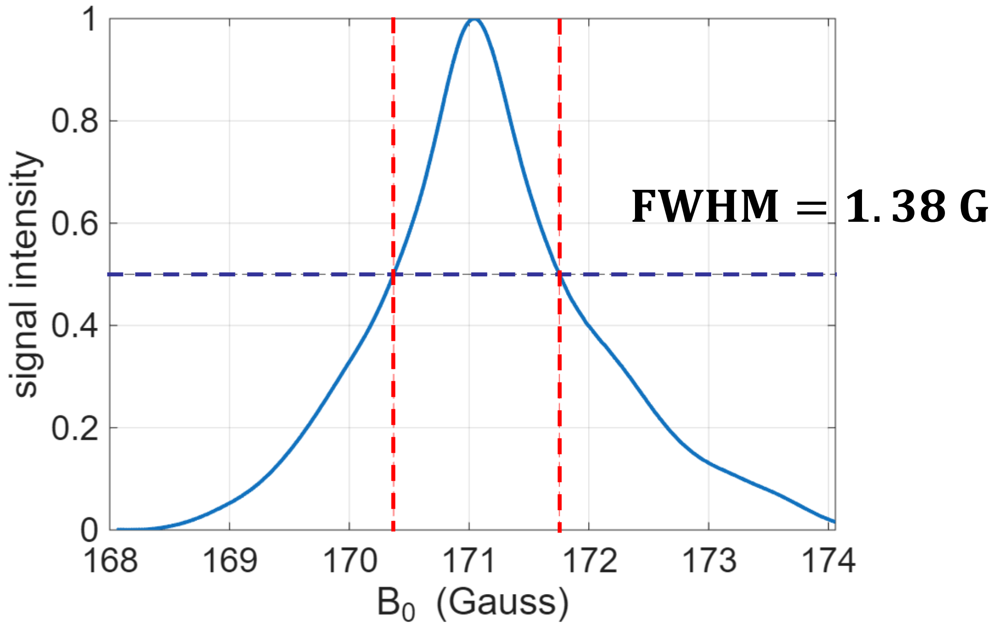

- Linewidth definitions based on Lorentzian absorption lineshape

$$\Delta B_{\mathrm{FWHM}}^{\mathrm{abs}} = 2\Gamma, \quad \Delta B_{\mathrm{pp}}^{\mathrm{der}} = 2/\sqrt{3}\,\Gamma$$

- $\Delta B_{\mathrm{pp}} = 774\ \mathrm{mG}$ (measured before midterm, pO_2 ~21%)

$\rightarrow \mathrm{FWHM} \approx 1.34\ \mathrm{G}$

$\rightarrow$ $\boxed{\text{relative error } \varepsilon \approx 2.9\%}$

- Spatial resolution:

$$\boxed{\Delta z_{res} \approx \frac{\Delta B_{pp}}{\mathrm{G_{max}}} = \frac{744\ \mathrm{mG}}{70\,\frac{\mathrm{uT}}{\mathrm{mm}}} = 1.1\ \mathrm{mm}}$$

SUMMARY AND OUTLOOK

Summary and outlook

- Summary
  - Compared with reported values in the literature, the achieved gradient strength is sufficient for EPR imaging.
  - Spatial–spatial and spectral–spatial imaging were both experimentally demonstrated, based on our VCO-PLL architecture.
  - Our VCO-based architecture is able to extract and reconstruct both spatial and spectral information of the EPR signal.
- Outlook
  - Employing a more suitable gradient driver (e.g. H-bridge based) to enable
    - larger and more stable gradient currents
    - extended projection angle range and improved spatial resolution
  - Further reduction of the gradient coil resistance, especially for the X-gradient, to
    - reduce thermal drift, improve current stability